PROBLEMY MECHATRONIKI
UZBROJENIE, LOTNICTWO, INŻYNIERIA BEZPIECZEŃSTWA

ISSN 2081-5891

8, 1 (27), 2017, 7-22

PROBLEMS OF MECHATRONICS
ARMAMENT, AVIATION, SAFETY ENGINEERING

Experimental and Finite Element Studies on Man-Rifle Reaction Force

Cyprian SUCHOCKI*, Janusz EWERTOWSKI

Warsaw University of Technology,
Department of Mechanics and Armament Technology,
85 Narbutta Street, 02-524 Warsaw, Poland
**Corresponding author's e-mail: c.suchocki@imik.wip.pw.edu.pl*

Received by the editorial staff on 24 July 2015.
The reviewed and verified version was received on 13 April 2016.

DOI 10.5604/01.3001.0009.8991

Abstract. The study concerns a man-weapon interaction during a gunshot. The recoil force measurements obtained for the Kalashnikov automatic rifle are presented and analyzed. The influence of shooter's mass, height and position is described. The breech pressure and projectile velocity data are presented as well. In addition, a finite element (FE) model of the shooter-rifle system is developed in order to qualitatively assess the quantities which could not be determined experimentally, i.e. the stress, strain and displacement fields which are generated in the human body due to the rifle recoil. Several conclusions are drawn that allow for better understanding of the recoil phenomenon and can be useful from the weapon designer's point of view.
Keywords: mechanics, firearm, recoil, muzzle rise, ballistics

1. INTRODUCTION

1.1. General

The recoil is one of the phenomena accompanying a gunshot. It occurs when a weapon and some parts of the shooter's body obtain a certain amount of kinetic energy as a consequence of the work performed by the gas pressure. This energy is later damped out by the dissipative forces acting both in the firearm and the human body.

In the published research results, a relatively large number of distinctions are made in order to assess the nature of the recoil. In fact, almost every researcher introduces his own rules of distinction and quantities aimed at measuring the recoil, e.g. [1, 2, 3, 4]. One of the utilized criteria characterizes the spatial motion performed by the weapon after firing a shot. Basically, two kinds of recoil can be distinguished this way, i.e.:

1. The horizontal recoil which refers to the firearm's translational motion in the direction which is opposite to the projectile's motion.
2. The vertical recoil, which may be further subdivided into pitch and yaw. The pitch, called the muzzle climb, muzzle rise or muzzle jump, refers to the upward rotational motion of the barrel. The term yaw is used to describe the angular displacement of the barrel occurring in the horizontal plane.

Another way of distinction, met in gun ballistics, is based on the projectile's position. Thus, one can distinguish:

1. The primary recoil, which takes place while the projectile is in the barrel;
2. The secondary recoil occurring after the projectile left the barrel.

For the subclasses of semi-automatic and automatic weapons one can also distinguish between:

1. The recoil, when the weapon components translate in the direction opposite to the projectile's motion;
2. The counter recoil referring to the motion of weapon components while they are returning to their initial position, taken prior to the time instant when the shot took place.

One may also adopt a different rule of distinction [3] which yields from the weapon's mechanical interaction with its immediate environment and different circumstances, i.e.:

1. The free recoil which takes place when the shots are fired without physical contact of the firearm and the shooter (for instance, when the firearm is hung up on strings or rests on a surface which may roll on the floor with negligible friction).

2. The suppressed recoil which takes place when the firearm is in contact with a part of human body (e.g. hand or arm) or some other sort of a compliant support. It results in the appearance of a reaction force which is exerted by the human organism on the weapon during a gunshot and shortly after it.

The problem of firearm-shooter interaction has been investigated for a long time, however still many questions are unanswered. There are several major reasons for the researchers' interest in the recoil phenomenon. One of them is the safety of the shooter who, as a result of the recoil, may sustain bruises or even injuries if the weapon is badly designed or if the acceptable limit of fired shots per day has been exceeded. The other reason is a serious decrease in shooting accuracy caused both by the muzzle jump and the man-rifle reaction force.

1.2. Present study

In this work, the suppressed recoil of the Kalashnikov automatic rifle is investigated. The experimental measurements of the human shoulder reaction force are presented. The experiments were performed employing shooters of different mass and height in order to determine the influence of these factors on the rifle recoil. Furthermore, the breech pressure and the projectile velocity were registered. To supplement the experimental studies, an FE model of the shooter-rifle system was developed. The FE simulation allows to qualitatively determine the stress, strain, and displacement fields inside the human body which could not be examined experimentally. Based on the conclusions drawn from both experimental and FE studies, a more complete description of the suppressed recoil phenomenon is obtained.

2. EXPERIMENTAL SETUP

The experiments were performed at the Ballistic Research Laboratory of Warsaw University of Technology. The experimental setup is depicted in Fig. 1. Both, the barrel and butt of a Kalashnikov rifle were modified in order to enable the installation of:

1. force sensors which were positioned in the rear of the firearm's butt;
2. a pressure sensor which was placed in the breech chamber, immediately over a hole drilled in the shell case;
3. a sensor that was applied at the muzzle and registered the time instant of projectile's exit.

All the utilized force sensors were piezoelectric load cells purchased at Kistler, Inc. Each sensor was equipped with its own charge amplifier connected to a digital recorder which collected the data.

The leaving muzzle sensor was developed at the Ballistic Research Laboratory. The sensor is an aluminum appliance which is fixed to the muzzle. It contains two copper wires. A passing projectile closes the electric circuit. As a consequence, a signal appears which marks the time instant at which the bullet exits the barrel.

Apart from the sensors mentioned above, a so-called velocity screen pair was utilized at each shot in order to measure the initial projectile velocity. The butt of the rifle was equipped with an additional element presented in Fig. 2. Two load cells, arranged at a certain distance, were utilized to measure the shoulder reaction force. This allowed for assessing the load distribution in the contact area. In order to determine the total recoil force, the data collected with both sensors were added up. The entire arrangement of the modified rifle butt is very stiff and was additionally checked prior to performing each of the shots. Thus, it was ensured that any motion of the recoil pad with respect to the stock was not possible.

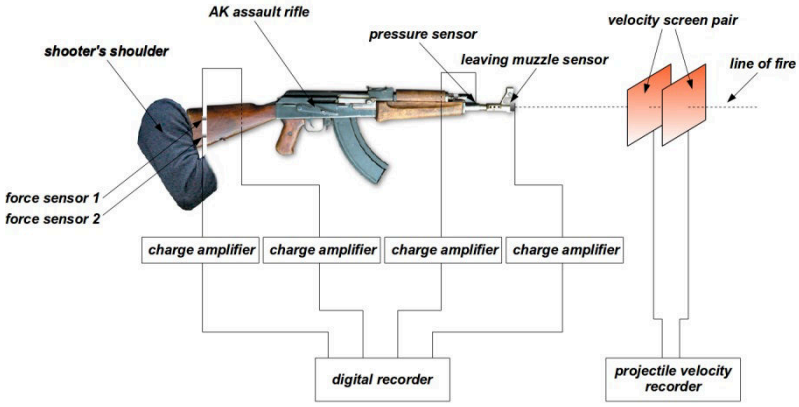

Fig. 1. Experimental setup

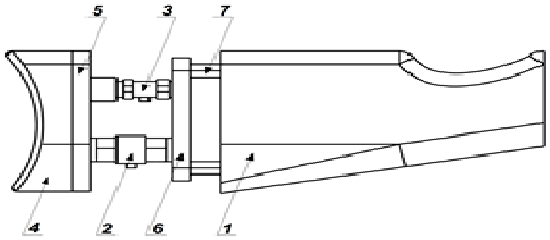

Fig. 2. Modified rifle butt: 1 – rifle butt, 2 – load cell model 9321, 3 – load cell model 9311, 4 – recoil pad, 5 – flat no. 1, 6 – flat no. 2, 7 – fixing

The total man-rifle reaction force is a sum of a static pre-load force and a dynamic component, i.e.:

$$F_{total}(t) = F_{static} + F_{dynamic}(t) \tag{1}$$

The dynamic component appears as a consequence of the shot and is a function of time, whereas the static component is a constant value. In the case of the Kalashnikov rifle, the static reaction force ranges from 200 to 350 N [3] and has little influence on the shooter's sensations.

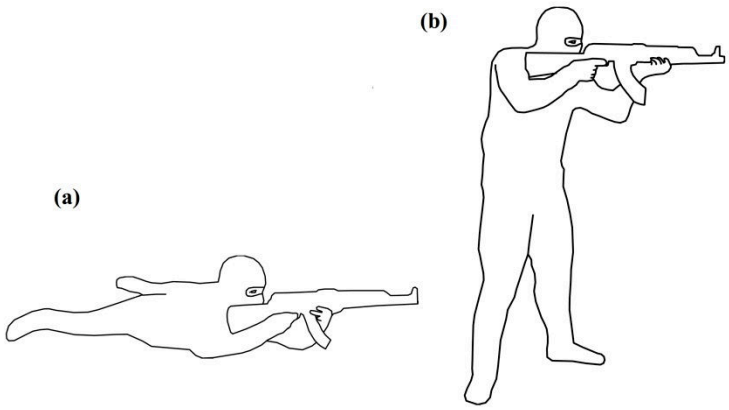

Fig. 3. Firing positions: (a) prone, (b) offhand

For the purpose of the measurements described in this study, the experimental apparatus was calibrated to show zero force value for the total man-rifle reaction force equal to F_{static}. In the following paragraph, the measurements of F_{dynamic} are gathered. In each case, the time instant at which the firing pin fires the primer is assumed as zero time.

Table 1. Shooter characteristics

Shooter	Weight [kg]	Height [cm]
A	60	165
B	88	185
C	90	190

Three different shooters participated in the experiments. Each of them was intentionally of different height and body mass which enabled to determine the influence of those factors on rifle's recoil. The masses and heights of the firers are gathered in Table 1. Every shooter fired three shots for the each of two firing positions (Fig. 3), i.e.:

1. the prone position,
2. the offhand position.

In each case, the force vs. time data obtained for three separate shots were further averaged. Thus, for every shooter and each firing position, an averaged force vs. time curve was obtained. During the shootings, the 7.62 × 39 mm M43 ammunition was used.

3. SHOULDER FORCE MEASUREMENTS

Regardless of the shooting position, generally two stages can be distinguished during the recoil of a Kalashnikov automatic rifle, cf [2], i.e.:

1. The initial stage, when the shoulder reaction force reaches its peak value while the force impulse is relatively small.
2. The second stage, when the magnitude of the shoulder reaction force is smaller, whereas its impulse is significant as it acts over a longer time period.

The both stages are separated by a short time period when the total recoil force drops below the value of the static pre-load. A similar two-stage character of the recoil was observed for other types of firearms [5, 6]. In all the cases considered below, the registered force data are presented separately for the two aforementioned stages. A solid vertical line marks the time instant at which the projectile exits the muzzle.

3.1. Prone position

In Fig. 4, the results obtained for the shooters A, B, and C shooting in prone position are shown. In the case of the first phase of the recoil (Figs. 4a, c, and e), the only noticeable differences are divergent maximum values of the shoulder reaction force along with the manner in which this force drops to zero. For the shooter A (weight 60 kg, height 165 cm), the maximum force is equal to 2.8 kN and is substantially greater than in the case of shooter C (weight 90 kg, height 190 cm, maximum force 2.4 kN). The situation is somewhat reversed during the second phase of the recoil (Figs. 4b, d, and f). The force values are smaller for the shooter A when compared to the shooter C. What is more, the shooter A brings the shoulder reaction force to zero at slightly faster pace than shooters B and C. One possible explanation for the last observation is that shooter A was more experienced in handling firearms.

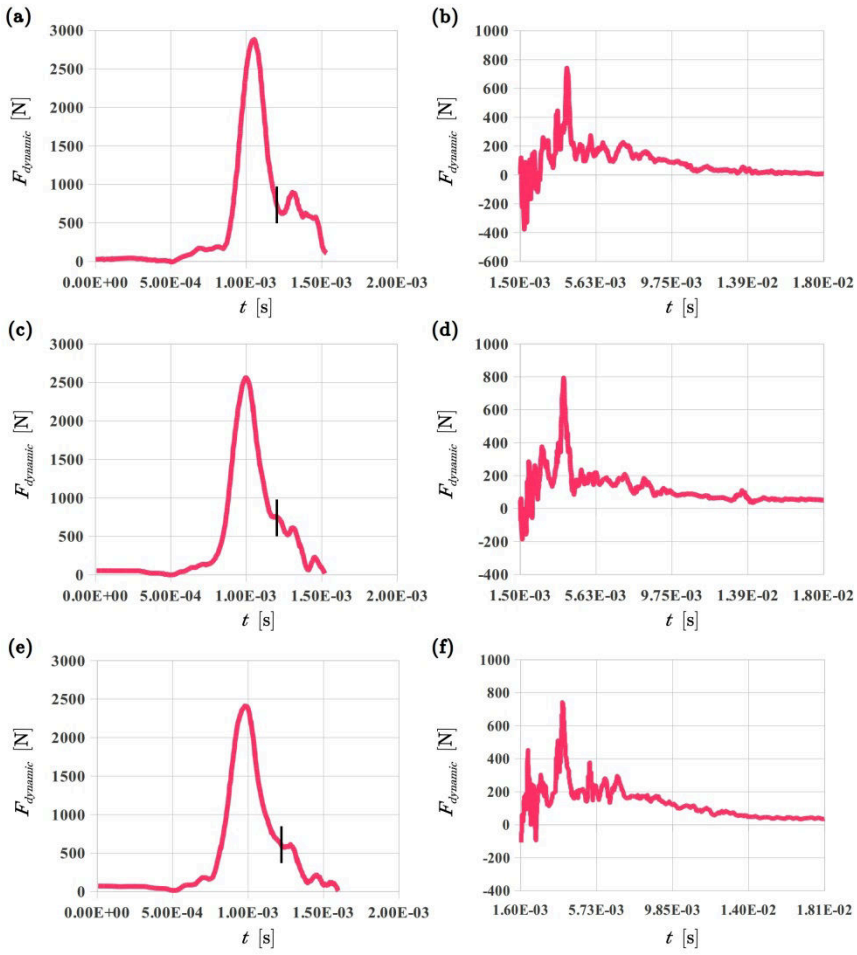

Fig. 4. Shoulder reaction force versus time (prone position):
(a) shooter A, stage one, (b) shooter A, stage two, (c) shooter B, stage one,
(d) shooter B, stage two, (e) shooter C, stage one, (f) shooter C, stage two

3.2. Offhand position

In Fig. 5, the results obtained for the shooters A, B, and C in shooting at the offhand position are shown. Comparing the force values measured for both shooting positions, one concludes that in the case of shooter A the maximum shoulder reaction force is about 300 N smaller for the offhand position, whereas in the case of shooter C the force increased by about 200 N for the offhand position. In the case of shooter B, the maximum shoulder reaction force value remains approximately the same regardless of the firing posture, i.e. about 2.5 kN.

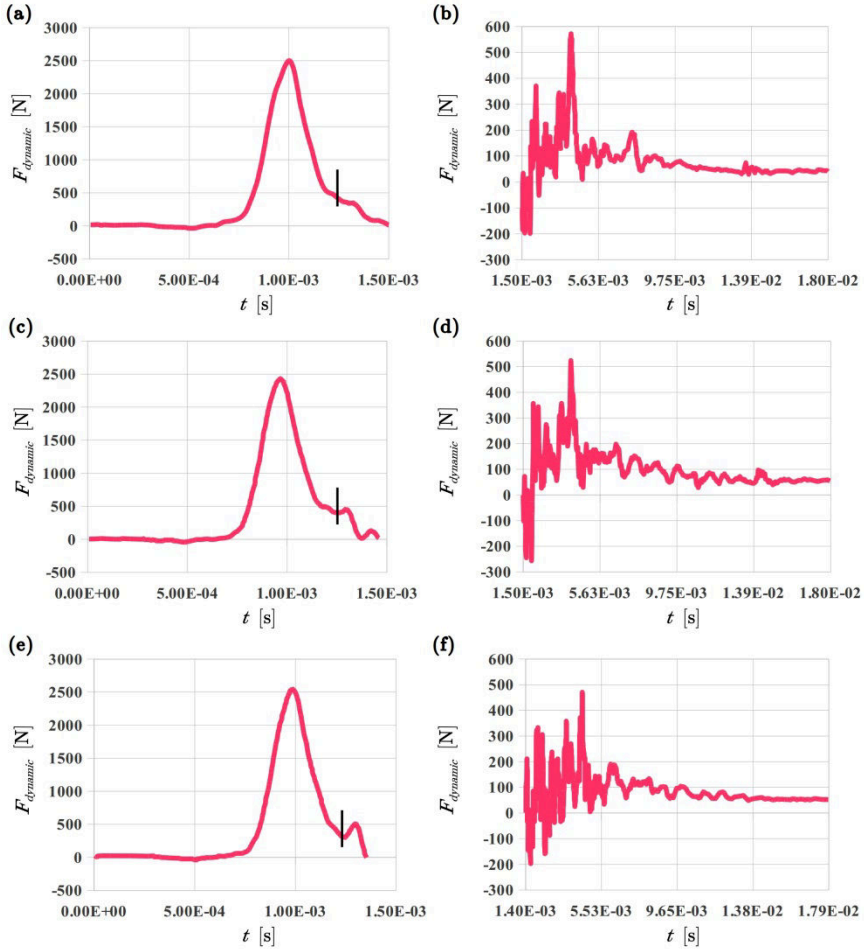

Fig. 5. Shoulder reaction force versus time (offhand position):
(a) shooter A, stage one, (b) shooter A, stage two, (c) shooter B, stage one,
(d) shooter B, stage two, (e) shooter C, stage one, (f) shooter C, stage two

Comparing the second recoil phase for both shooting positions, it is noticeable that the force is on average 100 N smaller in the case of offhand position. Furthermore, Figs. 5b, 5d, and 5f obtained for the offhand position have slightly more oscillatory character than Figs. 4b, d, and f. Some exemplary reaction force measurements collected independently by each of the load cells are shown in Fig. 6 (shooter A, prone position, both recoil stages).

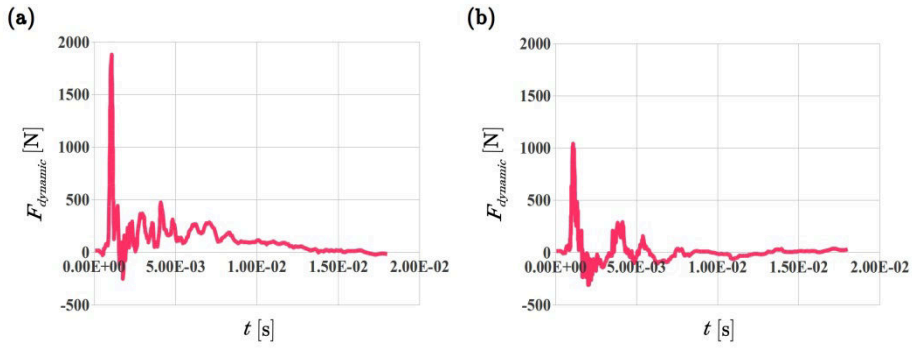

Fig. 6. Shoulder reaction force, shooter A, prone position:
(a) upper load cell, (b) lower load cell

4. FREE KINETIC ENERGY OF KALASHNIKOV RIFLE

In addition to the shoulder force measurements, the breech pressure and projectile exit velocity were registered. This allows calculating the free kinetic energy of Kalashnikov rifle. The following data were utilized:

- p_{max} = 281E6 Pa, – maximum breech pressure,
- p_{se} = 40.7E6 Pa, – shot exit pressure,
- l_w = 415.5E-3 m, – active bore length,
- d = 7.62E-3 m, – calibre,
- m_p = 8E-3 kg, – projectile mass,
- m_r = 3.89 kg, – rifle mass,
- m_ω = 1.63E-3 kg, – propellant mass,
- v_p = 730 m/s, – exit projectile velocity.

The rifle's kinetic energy before and after the projectile exits the barrel is computed using the following formulas, respectively [4]:

$$E_1 = \frac{(m_p + 0.5 \cdot m_\omega)^2 \cdot v_p^2}{2 \cdot m_r} \ldots;\ldots E_2 = \frac{(m_p + \beta \cdot m_\omega)^2 \cdot v_p^2}{2 \cdot m_r} \tag{2}$$

where β is the coefficient taking into account after-shot action of propellant gases:

$$\beta = \frac{6.45}{\left(\frac{p_{max}}{p_{se}} \cdot \frac{l_w}{d} \right)^{0.23}} \tag{3}$$

The values obtained from *E*qs (2-3) for the data listed above are: $E_1 = 5.32$ J, $E_2 = 7.83$ J, and $\beta = 1.65$. The calculated energy values are significantly different, however, they satisfy the free energy limit postulated in [4] for an automatic rifle, i.e. $T < 10$ J.

5. FINITE ELEMENT STUDY

The stress, strain, and displacement fields that are generated inside the human body during a gunshot cannot be determined experimentally. In order to qualitatively examine the distribution of aforementioned quantities and their propagation during a gunshot, an FE model was developed. The FE system Abaqus was utilized to perform the simulation.

5.1. Material properties

The human body is generally nonhomogeneous with various tissues such as bones, muscles, ligaments, tendons, and cartilage having different mechanical properties. Thus, for the sake of simplicity, it was decided to employ a homogenization framework that would allow treating the human flesh as a mechanically homogeneous and isotropic continuum. For that purpose, CAD models of a male human and a human skeleton (Fig. 7) obtained from [7] were utilized to determine the fraction of the total body volume occupied by the bone tissue.

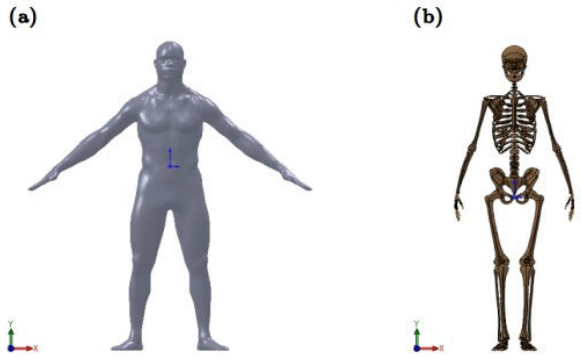

Fig. 7. Utilized CAD models: (a) shooter, (b) human skeleton

Having assessed the volume fractions of bone and soft tissues, the homogenization framework presented in [8] was used to determine the elasticity constants of human tissues.

The Young's modulus for bone tissue can be estimated utilizing Reuss homogenization method, i.e.

$$\frac{1}{E_b^R} = \frac{c_{cb}}{E_{cb}} + \frac{c_{sb}}{E_{sb}} \tag{4}$$

whereas, using Voigt method one obtains:

$$E_b^V = c_{cb} E_{cb} + c_{sb} E_{sb} \tag{5}$$

where c_{cb} and c_{sb} are the volume fractions of cortical and spongy bone, respectively. The Young's modulus of the cortical and spongy bone is denoted as E_{cb} and E_{sb}, respectively. According to Hill [9], the Young's modulus can be calculated as:

$$E_b = \frac{1}{2}(E_b^R + E_b^V) \tag{6}$$

Whereas the Poisson's ratio of bone tissue:

$$v_b = c_{cb} v_{cb} + c_{sb} v_{sb} \tag{7}$$

with v_{cb} and v_{sb} being the Poisson's ratios of cortical and spongy bone, respectively. Knowing the Young's modulus and the Poisson's ratio of the bone tissue, the elasticity constants of human flesh are calculated utilizing the same homogenization method, i.e.

$$\frac{1}{E_f^R} = \frac{c_b}{E_b} + \frac{c_{st}}{E_{st}} \tag{8}$$

and

$$E_f^V = c_b E_b + c_{st} E_{st} \tag{9}$$

where E_{st} is the Young's modulus of the soft tissues assumed to be equal to the Young's modulus of human cartilage, as recommended in [8]. The volume fractions of the bone and soft tissues are denoted as c_b and c_{st}, respectively. Accordingly, the Young's modulus of the human flesh is given as:

$$E_f = \frac{1}{2}(E_f^R + E_f^V) \tag{10}$$

and the Poisson ratio:

$$v_f = c_b v_b + c_{st} v_{st} \tag{11}$$

The constant values used for the homogenization have been gathered in Table 2.

Table 2. Material parameters of human tissues used in homogenization algorithm

Tissue	Volume fraction [-]*	Young's modulus [Pa]	Poisson's ratio [-]
Cortical bone	0.117	2E10	0.3
Spongy bone	0.883	1.5E9	0.46
Soft tissues	0.96	10.6E6	0.44

**The volume fractions of bone tissues are given with respect to the total volume of the bone tissue whereas the volume fraction of soft tissues is given with respect to the total volume of the human body.*

A linear viscoelastic model was assumed for the human flesh in order to take into account the strain rate dependency with the assumption that the volumetric deformations are purely elastic. The total Cauchy stress tensor is given as:

$$\sigma_{kl}(t)=s_{kl}(t)+p(t)\delta_{kl} \tag{12}$$

where δ_{kl} is the Kronecker delta, whereas s_{kl} and p is the stress deviator and volumetric stress, respectively, i.e.

$$s_{kl}(t)=\int_0^t 2G(t-\tau)\frac{\partial e_{kl}(\tau)}{\partial t}d\tau, \qquad p(t)=B\epsilon(t), \tag{13}$$

with e_{kl} being the deviator of the infinitesimal strain tensor ε_{kl}. Furthermore, the following relations hold:

$$s_{kl}=\sigma_{kl}-\frac{1}{3}\sum_{m=1}^{3}\sigma_{mm}\delta_{kl}, \qquad e_{kl}=\varepsilon_{kl}-\frac{1}{3}\sum_{m=1}^{3}\varepsilon_{mm}\delta_{kl} \tag{14}$$

$$p=\frac{1}{3}\sum_{k=1}^{3}\sigma_{kk}=\frac{1}{3}(\sigma_{11}+\sigma_{22}+\sigma_{33}), \qquad \epsilon=\sum_{k=1}^{3}\varepsilon_{kk}=\varepsilon_{11}+\varepsilon_{22}+\varepsilon_{33} \tag{15}$$

The deviatoric relaxation function is assumed in the form of a single Prony term, i.e.:

$$G(t)=\frac{G_\infty}{1-g_1}\left[1-g_1\left(1-e^{-t/\tau_1}\right)\right], \quad G_\infty=\frac{E_\infty}{2(1+\nu)}, \quad B=\frac{E_\infty}{3(1-2\nu)} \tag{16}$$

where $E\infty$ is the long-term Young's modulus of the human flesh which, along with the Poisson's ratio ν, were calculated utilizing the homogenization technique described above. The relaxation coefficient g_1 and the relaxation time τ_1 were calibrated empirically.

The linear elastic properties were assumed for both steel and beech wood which the rifle stock is made of. The material parameter' values used in the FE simulation are listed in Table 3.

Table 3. Material parameter values used in FE simulation

Material	Mass density [kg/m3]	Young's modulus [Pa]	Poisson's ratio [-]	Relaxation coefficient [-]	Relaxation time [s]
Human flesh	1000	6.44E7	0.44	0.955	1E-4
Steel	1800*	2.1E11	0.35	-	-
Beech wood	600	1.57E10	0.35	-	-

**An equivalent mass density was calculated for steel as the total mass of steel rifle components divided by their total volume.*

5.2. Boundary conditions

A CAD model of the Kalashnikov automatic rifle was created and attached to the modified version of human model shown in Fig. 8a in order to mimic a shooter in an offhand shooting position. Both CAD models were meshed using tetrahedral elements, cf Figs 9a-c.

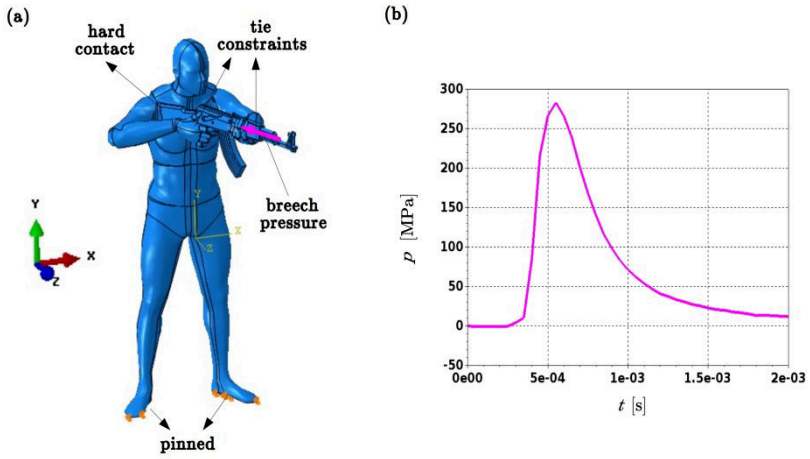

Fig. 8. Boundary conditions: (a) constraints and external loads, (b) breech pressure multilinear curve

The defined constraints and boundary conditions are depicted in Fig. 8a. A "hard contact" option available in Abaqus/Explicit package was used to define contact between the human shoulder and the rifle butt.

In the areas where shooter's hands contact the rifle, "tie" constraints were defined. For the lower surfaces of shooter's feet, the displacements were set to equal zero. The breech pressure was applied to the bolt surface. The experimental breech pressure data were utilized to define a multilinear curve characterizing how pressure changes over time, cf Fig. 8b.

5.3. Simulation results

The FE simulation results are depicted in Figs. 9d-f.

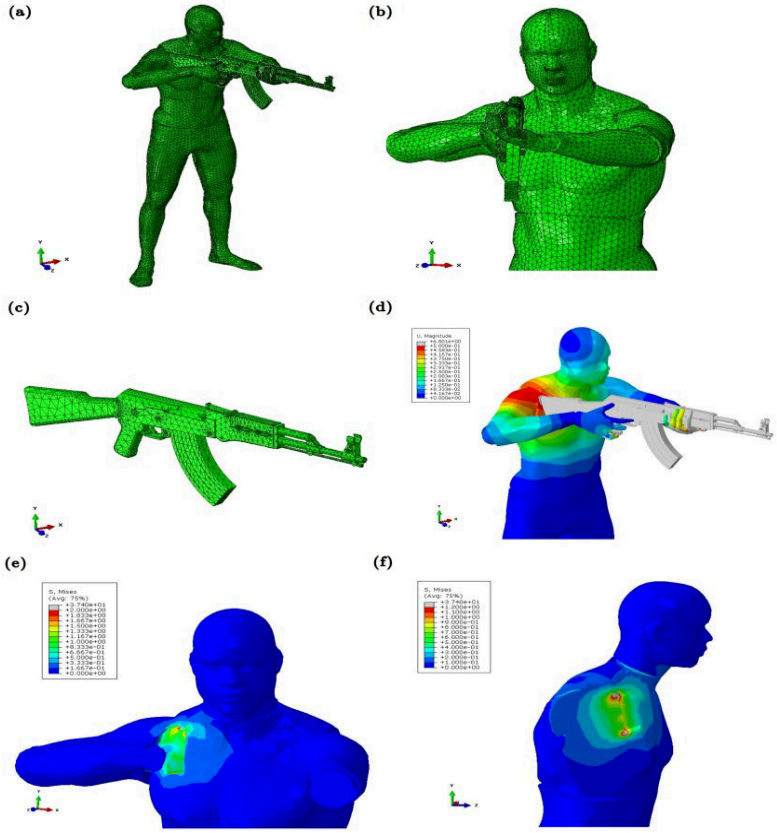

Fig. 9. FE study: (a) model, (b) model – close up, (c) Kalashnikov rifle model, (d) distribution of displacement magnitude at $t = 2$ ms, (e) distribution of HMH stress at $t = 1$ ms – front view, (f) distribution of HMH stress at $t = 1$ ms – side view

The analysis of the results allows one to make the following observations:

- The equivalent Huber-Mises-Hencky (HMH) stress contour plot in the shoulder-rifle butt contact area is similar to the one known from the contact problem for an elastic half-space indented by a rigid stamp, cf Fig. 8f. The average stress value in the immediate vicinity of the contact surface is about 1.0 MPa. However, stress concentrations are observed near both upper and lower part of the rifle butt. In those areas, the HMH stress ranges up to 37.4 MPa.
- A spherical stress wave is observed propagating through the human body during a gunshot. The centre of the wave is situated in the area where human shoulder touches the rifle butt.
- The magnitude of the principal strain in the contact area is no greater than 1.0%. Thus, the infinitesimal strain theory is sufficient for the analysis of human-rifle contact.

6. CONCLUSIONS

By combining the experimental and numerical results presented in this study, the following conclusions can be drawn:

1. A comparison of the shoulder reaction force data for both the prone and offhand positions (Figs. 4 and 5) reveals that the force value registered for the prone position is usually higher than in the case of the offhand position. The most sensible explanation for this result is that the prone shooting position is characterized by a higher stiffness of the shooter-rifle system.
2. The shoulder reaction force plot during the first 2 ms of the recoil is a replication of the breech pressure versus time profile. The force peak is retarded by 0.3 ms only when compared to the breech pressure maximum, cf e.g. Figs. 5c and 7b.
3. As discussed earlier, the shoulder force data were collected by two load cells as depicted in Fig. 2. In Fig. 6, exemplary plots of forces registered by the upper and the lower sensors are shown. It can be seen that the upper load cell registered a substantially greater force values than the lower load cell. This observation is in an agreement with the FE results, where higher stress values can be seen in the upper region of the shoulder-rifle contact area, cf Figs. 9e, f.
4. It is important to take into account that apart from the rifle itself, the shooter's hands and arms are subjected to muzzle climb as well. The mass centre of the system comprising the firearm, the shooter's hands, and arms is situated below the shoulder-rifle butt contact area. Thus, the breech force and the shoulder reaction force generate couples of different signs with respect to the system's mass centre, i.e. the breech force causes the muzzle climb while the shoulder reaction force opposes it.

This hypothesis is supported by the data published in [3] where it was demonstrated that Kalashnikov rifle's rotation begins when the shoulder reaction force dynamic component is equal to zero, whereas the breech force is nonzero with about 20.0% of its maximum magnitude.

The results presented in this work contribute to the current state of art in the firearm recoil theory. One can expect that better understanding of the processes accompanying a gunshot will allow for a reduction of negative phenomena such as horizontal and vertical recoil in the new weapon designs.

REFERENCES

[1] Chodkiewicz Leon. 1956. *Effect of firearm's recoil on shooter* (in Polish). Journal of Special Technology, vol. 2, Warsaw, Poland: Institute of Precision Mechanics.

[2] Ewertowski Janusz. 2007. „The analysis of humeral weapons interaction strength on the shooter during the shot" (in Polish). *Bulletin of Military University of Technology* 56 : 207-222.

[3] Kochański Stanisław. 1979. *Suppressed recoil of shoulder-fired weapons* (in Polish). Scientific Surveys of the Institute of Mechanical Equipment Design, 2. Warsaw, Poland: Warsaw University of Technology.

[4] Wilniewczyc Piotr. 1958. *Automatic weapons* (in Polish). Warsaw, Poland: Ministry of Defence.

[5] Kijewski Jacek, Łukasz Szmit. 2013. „Theoretical and experimental studies on the recoil of automatic firearms" (in Polish). *Problemy Mechatroniki. Uzbrojenie, lotnictwo, inżynieria bezpieczeństwa - Problems of Mechatronics, Armament, Aviantion, Safety Technology* 4 : 49-66.

[6] Ewertowski Janusz, Robert Piekarski. 2016. „The impact of selected sorts of rifles on shooter – comparative analysis". *Problems of Armament Technology* 138 : 73-86.

[7] https://grabcad.com/ (2016).

[8] Chigarev V. Anatoly, Andrey V. Borisov. 2011. "Simulation of controlled motion of the bipedal antropomorphic mechanism". *Russian Journal of Biomechanics* 15 : 69-83.

[9] Hill Rodney, *The mathematical theory of plasticity*, Oxford University Press, New.